

GT2011-45- \$'

ANALYSIS OF THE EFFECTS OF PARALLEL AND ANGULAR MISALIGNMENT IN HYPERSTATIC ROTORS EQUIPPED WITH OIL-FILM BEARINGS

P. Pennacchi, A. Vania, S. Chatterton

Politecnico di Milano, Dept. of Mechanical Engineering
Via La Masa, 1, I-20156, Milano, Italy

ABSTRACT

Misalignment is one of the most common sources of trouble of rotating machinery having couplings between the shafts. Ideal alignment is a chimera and the coupling flanges of the shafts are never ideally aligned, presenting angular and/or parallel misalignment (defined also as radial misalignment or offset). In particular, during the shaft rotation, if coupling misalignment between the shafts of a statically aligned line is excessive, a periodical change, of the load on the bearings in hyperstatic shaft-lines, occurs. If the rotating machine is equipped with oil-film bearings, the change of the loads on the bearings causes also the variation of their oil-film dynamic characteristics, i.e. damping and stiffness, and the complete system cannot be considered as linear.

In the paper, this phenomenon is modelled accurately and analyzed by considering the simulated response of a misaligned rotor train in the time domain. A finite element model is used for the hyperstatic rotor, while bearing characteristics are calculated by integrating Reynolds equation (considering the actual type and dimensions of the bearings) as a function of the instantaneous load acting on the bearings, caused by the coupling misalignment. Nonlinear effects are highlighted and the spectral components of system response are analyzed, in order to give pertinent diagnostic information.

INTRODUCTION

Rotor misalignment is considered as the second most common malfunction after unbalance, as observed by Muszyńska [1], which remarked also that this interesting topic has not been object of much attention by researchers.

The authors share this position and want to contribute by presenting a paper aimed at explaining the reason of the presence of super-harmonic components, i.e. of nonlinear behaviour, in rotor vibration spectrum as a consequence of rigid coupling misalignment, owing to wrong assembly or of

imperfect flange machining, of a hyperstatic shaft-line equipped with journal bearings.

Various kinds of rotor misalignment are analyzed in literature. Some papers consider the misalignment of the journal with respect to the bearing, without dealing with the complete dynamics of the shaft-line; an example is given by Bou-Saïd and Nicolas [2]. The causes of the misalignment in rotating machinery are discussed by Bently [3], which also mentions the additional loading on the bearings, but does not present any mathematical model on the matter. Xu and Marangoni [4-5] studied the misalignment of a flexible coupling, highlighting the similarities with universal joint operation and the presence of 2X component in the vibration spectrum. In that study, the shaft-line was supported by ball bearings and the cause of the 2X component was ascribed to the presence of the variable stiffness of the flexible coupling as a consequence of the misalignment. Often papers in literature report that misalignment causes 2X components, but they neither consider the type of joint nor the type of the bearings. Also Sekhar and Prabhu [6] considered flexible coupling, used Gibbons' theoretical model [7] and performed some simulations in which 2X components were evident. Lee and Lee [8] used a test rig, equipped by ball bearings and flexible coupling, to verify the results of their theoretical model and observed the results on the orbit shape. Hu et al. [9] designed a test rig with flexible rotors equipped by three or more journal bearings suitable to study the misalignment. However, in this case, the focus is on "lateral misalignment" of the supports, rather than on coupling misalignment. Al-Hussain and Redmond [10] presented a theoretical model of two coupled Jeffcott rotors supported on rigid bearings. Radial misalignment was simulated and only 1X component resulted in the lateral vibration steady-state spectra. They observed also excitation of torsional vibrations. Al-Hussain proposed a further model about angular misalignment [11] affecting the flexible joint

connecting two Jeffcott rotors installed on journal bearings. In this case only stability conditions were analyzed.

Lees [12] observed that the term “misalignment” is used to label several situations corresponding to different physical processes and the authors agree also with this point of view. He focused his interest on rigid couplings, introducing a simple model that considers orientation and different tightening of the coupling bolts and neglects the presence of journal bearings. Nonlinear system response resulted as a consequence of coupling between torsional and lateral vibrations. Tsai and Huang [13] used a transfer matrix to model radial misalignment and found results similar to [10], even if they gave different motivations to the presence of 1X component only. More recently, Balahoo et al. [14] studied speed transients of a misaligned rotor with a simplified model. On the contrary, the model presented hereafter by the authors is suitable to study the behaviour of real rotating machinery, considering all the possible features.

From the analysis of the current literature it results that a complete analysis of the dynamic effect of rigid coupling misalignment on a real shaft line, i.e. a hyperstatic rotor with several bearings and couplings, is lacking. In this paper, the authors propose a complete and original method to simulate the behaviour of real shaft line, supported by several oil-film bearings, with rigid coupling misalignment. Nonlinear effects are highlighted and the spectral components of system response are analyzed, in order to give pertinent diagnostic information.

MODEL OF COUPLING MISALIGNMENT

Let's consider a hyperstatic shaft-line, like that represented in Fig. 1, which is composed by three different rotors, connected by two rigid couplings. In particular, the first rotor is the HP-IP (high pressure – intermediate pressure) turbine, the second is the LP (low pressure) turbine and the last one is the generator. The model proposed is anyway applicable for other types of machines, with different number of couplings or rotor bearings.

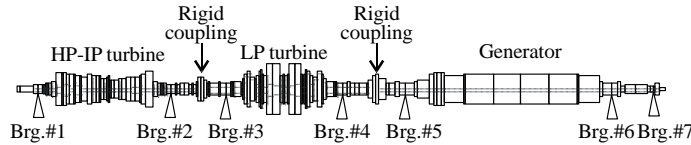


Fig. 1. Hyperstatic shaft-line.

The shaft-line is modelled in a standard way by means of a finite beam model and rigid disks, considering only the lateral vibrations, and 4 degrees of freedom (d.o.f.s) - two translational and two rotational - are considered per each node (see Fig. 2). On the contrary, axial and torsional vibrations will be neglected. Considering the general j^{th} element of the shaft-line, the generalized displacement vector $\mathbf{x}_j^{(r)}$ of the j^{th} rotor node is ordered as follows:

$$\mathbf{x}_j^{(r)} = \{x_j^{(r)} \quad \mathcal{G}_{x_j}^{(r)} \quad y_j^{(r)} \quad \mathcal{G}_{y_j}^{(r)}\}^T \quad (1)$$

Two subsequent nodes, the j^{th} and the $(j+1)^{\text{th}}$, define the j^{th} element of the machine. Index j is the main index used to order shaft nodes and elements. If the shaft has n_r nodes, thus $n_r - 1$ elements, the vector $\mathbf{x}^{(r)}$ of the generalized displacements of all the rotor nodes is composed by all the ordered vectors $\mathbf{x}_j^{(r)}$, as shown in Eq. (2):

$$\mathbf{x}^{(r)} = \{x_1^{(r)} \quad \mathcal{G}_{x_1}^{(r)} \quad y_1^{(r)} \quad \mathcal{G}_{y_1}^{(r)} \cdots x_{n_r}^{(r)} \quad \mathcal{G}_{x_{n_r}}^{(r)} \quad y_{n_r}^{(r)} \quad \mathcal{G}_{y_{n_r}}^{(r)}\}^T \quad (2)$$

The mass matrix of the coupled rotors $[\mathbf{M}^{(r)}]$, which takes also into account the secondary effect of the rotatory inertia, the internal damping matrix $[\mathbf{C}^{(r)}]$, the stiffness matrix $[\mathbf{K}^{(r)}]$, which takes also into account the shear effect, and the gyroscopic matrix $[\mathbf{G}^{(r)}]$, all of order $(4n_r \times 4n_r)$, can be defined by means of standard Lagrange's methods, considering beam elements and rigid disks, as shown e.g. in [15-16]. Damping and gyroscopic matrices will be used in the following for the dynamic simulations.

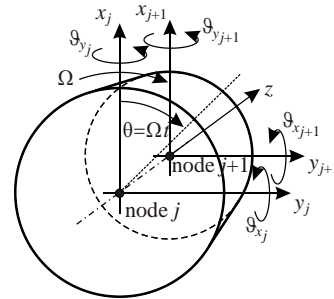


Fig. 2. General rotor element.

The shaft-line is supported on n_b oil-film bearings. They are located in correspondence of some nodes of the shaft, which are labelled by the indexes belonging to the set:

$$I_c = \{j_{\text{Brg.\#1}} \quad \cdots \quad j_{\text{Brg.\#n_b}}\} \quad (3)$$

Shaft nodes whose indexes belong to I_c are defined as *constrained nodes* and indicated as $\mathbf{x}_c^{(r)}$, while the remaining nodes are the *free nodes* $\mathbf{x}_f^{(r)}$:

$$\mathbf{x}_c^{(r)} = \mathbf{x}_{j \in I_c}^{(r)}; \quad \mathbf{x}_f^{(r)} = \mathbf{x}_{j \notin I_c}^{(r)} \quad (4)$$

During the machine installation, the shaft-line is statically aligned, using several methods like those described in [17], in order to have null static bending moments on the rigid coupling flanges. This is realized by displacing the supports in vertical directions, so that elements of $\mathbf{x}_c^{(r)}$ are generally not all null. The static centreline is a catenary. If rigid couplings were also ideally aligned, without any radial or angular misalignment on their flanges, the static reaction forces on the bearings could be calculated, in order to determine the oil-film dynamic characteristics.

Otherwise, like described in this paper, it is necessary to take into account the effect of rigid coupling misalignment on the static centreline and, as a consequence, on the reactions of the bearing, considering that these reactions are changing due

to the rotation of the shaft, i.e. to the orientation of the misalignment with respect to the phase reference.

Effect of rigid coupling misalignment on the shaft-line

Let's consider Fig. 3 in which a close up of a rigid coupling of the machine is shown. For the sake of simplicity, only a coupling is considered, being the model presented easily generalizable to n_c couplings. In the general case, the coupling faces are connected in correspondence of the j_c^{th} node and both radial and angular misalignment may occur as a consequence of wrong mounting or imperfect machining. However, not only the magnitudes of these misalignments have to be considered, but also the relative phase with respect to the phase reference and the fact that the shaft is rotating with rotational speed Ω . Thus both types of misalignments are conveniently represented by means of vectors, using for simplicity a complex notation [18]:

$$\begin{aligned} \text{angular misalignment: } & \Delta\alpha e^{i\varphi_\alpha} e^{i\Omega t} \\ \text{radial misalignment: } & \Delta r e^{i\varphi_r} e^{i\Omega t} \end{aligned} \quad (5)$$

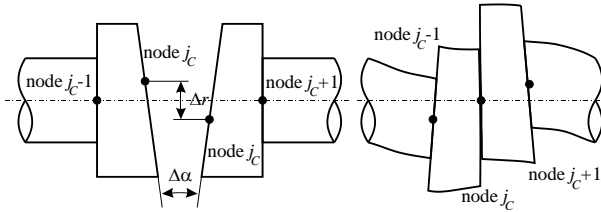


Fig. 3. Scheme of the coupling misalignment.

Therefore, the effect of the rigid coupling misalignment is to impose generalized displacements $\Delta \mathbf{x}_j(\theta)$, which are function of the angular position $\theta = \Omega t$ of the shaft, on the d.o.f.s corresponding to the j_c^{th} coupling node. Vector $\Delta \mathbf{x}(\theta)$ has the same size of $\mathbf{x}^{(r)}$, because the d.o.f.s not corresponding to coupling nodes are set equal to 0.

Calculation of the static reactions on the bearings

The static reactions $\mathbf{R}(\theta)$ on the bearings can be calculated by imposing the static equilibrium of the free-body shaft-line and considering the imposed shaft alignment conditions, that is:

$$\begin{aligned} [\mathbf{K}^{(r)}] (\mathbf{x}^{(r)} + \Delta \mathbf{x}(\theta)) + \mathbf{W} &= \mathbf{R}(\theta) \rightarrow \\ [\mathbf{K}^{(r)}] \mathbf{x}^{(r)} + [\mathbf{K}^{(r)}] \Delta \mathbf{x}(\theta) + \mathbf{W} &= \mathbf{R}(\theta) \rightarrow \\ [\mathbf{K}^{(r)}] \mathbf{x}^{(r)} + \mathbf{F}_c(\theta) + \mathbf{W} &= \mathbf{R}(\theta) \end{aligned} \quad (6)$$

where \mathbf{W} is the weight force vector that can be calculated as:

$$\mathbf{W} = [\mathbf{M}^{(r)}] \{-g \ 0 \ 0 \ 0 \dots -g \ 0 \ 0 \ 0\}^T \quad (7)$$

and $\mathbf{F}_c(\theta)$ is the *equivalent force* due to the coupling misalignment. The only elements of vector $\mathbf{F}_c(\theta)$ that are different from zero are those corresponding to the d.o.f.s of j_c^{th}

node and can be calculated by considering the stiffness sub-matrix corresponding to the j_c^{th} node:

$$\mathbf{F}_c \Big|_{j=j_c} = [\mathbf{K}^{(r)}] \Big|_{j=j_c} \begin{bmatrix} 1 & 0 \\ 0 & i \\ i & 0 \\ 0 & 1 \end{bmatrix} \begin{Bmatrix} \Delta r e^{i\varphi_r} \\ \Delta\alpha e^{i\varphi_\alpha} \end{Bmatrix} e^{i\theta} \quad (8)$$

After these considerations, Eq. (6) can be re-written by reordering the d.o.f.s of the nodes and grouping the free and the constrained ones:

$$\begin{bmatrix} \mathbf{K}_{ff}^{(r)} & \mathbf{K}_{fc}^{(r)} \\ \mathbf{K}_{cf}^{(r)} & \mathbf{K}_{cc}^{(r)} \end{bmatrix} \begin{Bmatrix} \mathbf{x}_f^{(r)} \\ \mathbf{x}_c^{(r)} \end{Bmatrix} + \begin{Bmatrix} \mathbf{W}_f \\ \mathbf{W}_c \end{Bmatrix} + \begin{Bmatrix} \mathbf{F}_{c_f}(\theta) \\ \mathbf{0} \end{Bmatrix} = \begin{Bmatrix} \mathbf{0} \\ \mathbf{R}(\theta) \end{Bmatrix} \quad (9)$$

since, obviously, $\mathbf{F}_c(\theta) = \mathbf{0}$.

The static free displacements as function of the angular position θ of the shaft are obtained as:

$$\mathbf{x}_f^{(r)}(\theta) = -[\mathbf{K}_{ff}^{(r)}]^{-1} \left([\mathbf{K}_{fc}^{(r)}] \mathbf{x}_c^{(r)} + \mathbf{W}_f + \mathbf{F}_{c_f}(\theta) \right) \quad (10)$$

and the reactions on the bearings as:

$$\mathbf{R}(\theta) = [\mathbf{K}_{cf}^{(r)}] \mathbf{x}_f^{(r)} + [\mathbf{K}_{cc}^{(r)}] \mathbf{x}_c^{(r)} + \mathbf{W}_c \quad (11)$$

Notice that, as a consequence of the presence of the coupling misalignment, the reactions of Eq. (11) have generally both the vertical and the horizontal components and that they are 1X periodical.

Calculation of the oil-film dynamic characteristics

It is commonly agreed that the static reactions on the bearings are used as the input loads to calculate the oil-film dynamic characteristics, being that static reactions are largely predominant on the dynamical ones, due for instance to unbalances. However, in the case considered in the paper, as a consequence of the presence of the coupling misalignment, the loads are not constant and depend on the angular position θ of the shaft, see Eq. (11). Hence, also the dynamic characteristics of the oil-film in the bearings have to be calculated as a function of θ . For the sake of simplicity, only constant rotational speeds will be taken into account.

Therefore, starting from the actual type and geometry of each one of the n_b bearings, Reynolds equation in the isoviscous form [19-20] is used:

$$\frac{\partial}{\partial \xi} \left(\frac{h^3}{\eta} \frac{\partial p}{\partial \xi} \right) + \frac{\partial}{\partial \zeta} \left(\frac{h^3}{\eta} \frac{\partial p}{\partial \zeta} \right) = 6U \frac{\partial h}{\partial \xi} + 12W \quad (12)$$

where ξ is the coordinate in the sliding direction, ζ that in the axial direction, η the dynamic viscosity, h the film thickness, p the pressure, U the entraining velocity and W the squeeze velocity. Equation (12) is then expressed in non-dimensional form. Effect of small displacements and squeeze velocities are also introduced.

The integration of Reynolds equation is performed by using finite difference and the journal static equilibrium position is found that is balancing the reactions $\mathbf{R}(\theta)$ in an iterative way. Dynamic fluid film forces $\mathbf{F}_b(\theta)$ are then calculated by using the method of the perturbation of equilibrium position.

SIMULATION OF SHAFT-LINE DYNAMICAL BEHAVIOUR

In order to perform the simulation of the dynamical behaviour of the shaft-line at the operating speed, a dynamical model should be set-up. The matrices of the coupled rotors have been already introduced and now the effects owing to the foundation dynamics and to the oil-film forces are accounted for.

Different methods can be used to model the foundation. For the sake of brevity, only pedestals, i.e. lumped 2 d.o.f.s systems, will be considered. A discussion about other methods (modal or rigid) is reported in [21]. In a similar manner to the rotor, also the d.o.f.s of the foundation, horizontal and vertical displacements, which are connected by the n_b bearings to the rotor, can be ordered in a vector:

$$\mathbf{x}^{(f)} = \{x_1^{(f)} \quad y_1^{(f)} \dots x_{n_b}^{(f)} \quad y_{n_b}^{(f)}\}^T \quad (13)$$

The complete vector of the generalized displacements of the system is therefore:

$$\mathbf{x} = \{\mathbf{x}^{(r)} \quad \mathbf{x}^{(f)}\}^T \quad (14)$$

The structure of $[\mathbf{M}^{(f)}]$, $[\mathbf{C}^{(f)}]$ and $[\mathbf{K}^{(f)}]$ is not relevant in this paper and depends on how the supporting structure is implemented, see [21].

The remaining external forcing systems acting on the rotor are the weight \mathbf{W} and the residual unavoidable unbalance distribution, which will be taken into account by the *equivalent unbalance* in the j_u^{th} node:

$$\mathbf{F}_u(t) = \{0 \quad ; \quad 1 \quad 0 \quad i \quad 0 \quad ; \quad 0\}^T m_u r_u \Omega^2 e^{i\varphi_u} e^{i\Omega t} \quad (15)$$

By considering all the external forcing and Eq. (6), the fully assembled system of equations is nonlinear, because many terms of it depends on the angular position $\theta = \Omega t$:

$$\begin{aligned} [\mathbf{M}] \ddot{\mathbf{x}} + ([\mathbf{C}] + \Omega[\mathbf{G}]) \dot{\mathbf{x}} + [\mathbf{K}] \mathbf{x} = \\ = -\bar{\mathbf{F}}_C(\theta) - \bar{\mathbf{W}} + \bar{\mathbf{F}}_u(t) + \mathbf{F}_b(\theta) \end{aligned} \quad (16)$$

where the over-bars indicate that the corresponding vectors are padded with zeros on the foundation d.o.f.s, and the matrices are those of the fully assembled system.

The nonlinear system of equations in Eq. (16) is integrated in the time domain using the Newmark's implicit method, in which all the quantities depending on θ are evaluated for each integration step.

Simulation results

The model of the machine, used to show the results obtained with the described method, is relative to a steam turbo-generator unit of about 320 MVA, already sketched in Fig. 1. Node number is equal to 175 and bearing #1, #2 and #7 are of tilting pad type, while the others of 2-lobes type.

The system response is calculated at the operating speed of 3000 rpm, considering also the presence of an unbalance on about the mid of the LP turbine (0.3 kgm with phase 0°). Different combinations of radial and angular misalignment conditions of the rigid coupling between HP-IP and LP turbines have been analysed. An example is shown in Figs. 4-7, where only the shaft orbits, in nodes corresponding to the vibration measuring planes close to the bearings #1-#4 of the actual machine, are shown. In this case, radial misalignment of $100 \mu\text{m}$ @ 90° and angular misalignment of 15 mrad @ 0° have been applied.

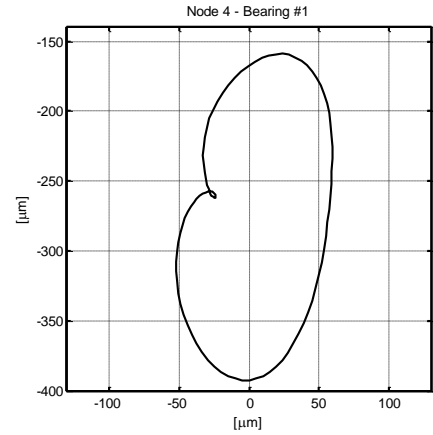


Fig. 4. Rotor orbit close to Brg. #1, Rad. Mis. $100 \mu\text{m}$ @ 90° , Ang. Mis. 15 mrad @ 0° .

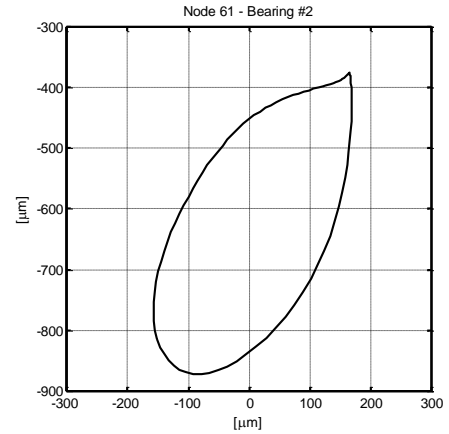


Fig. 5. Rotor orbit close to Brg. #2, Rad. Mis. $100 \mu\text{m}$ @ 90° , Ang. Mis. 15 mrad @ 0° .

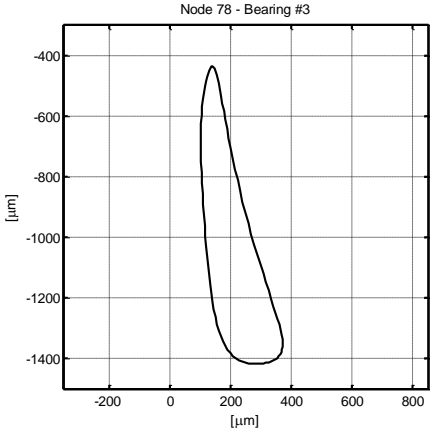


Fig. 6. Rotor orbit close to Brg. #3, Rad. Mis. 100 μm @ 90°, Ang. Mis. 15 mrad @ 0°.

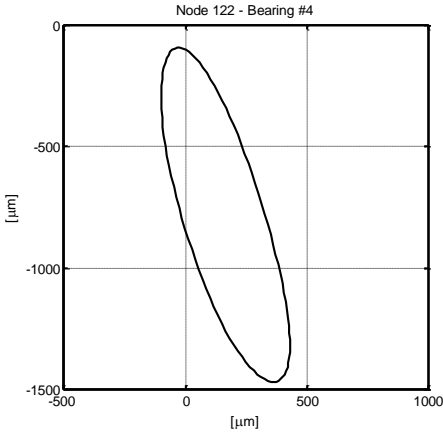


Fig. 7. Rotor orbit close to Brg. #4, Rad. Mis. 100 μm @ 90°, Ang. Mis. 15 mrad @ 0°.

Orbits in generator bearings are less affected by the misalignment and are not shown. Similarly, the orbits in the other nodes of the rotor are not displayed both for the sake of brevity and because they are never measured in the practice.

The case considered is already critical and vibration amplitudes would be dangerous for the actual rotating machine, because the bearing clearance would be exceeded. Orbits, in the measuring planes close to bearings #1 - #3, show rather clearly the presence of super-harmonics components (owing to the deformed shape respect to the elliptical one) and the presence of nonlinear effects. These considerations are clearer if vibration spectra are considered and Figs. 8-11 show the corresponding ones to the orbits close to bearings from #1 to #4.

Even though a logarithmic scale is used for the amplitudes, it is easy to observe that at least 2X and 3X components have remarkable amplitudes (i.e. measurable, the horizontal dashed lines in the figures indicate the amplitude of 1 μm in the HP-IP bearings and the LP one close to the rigid coupling. Bearing #4 is rather “far” from the rigid coupling and does not “feel” so

much the effect of the misalignment: higher harmonic components are much smaller than the 1X component.

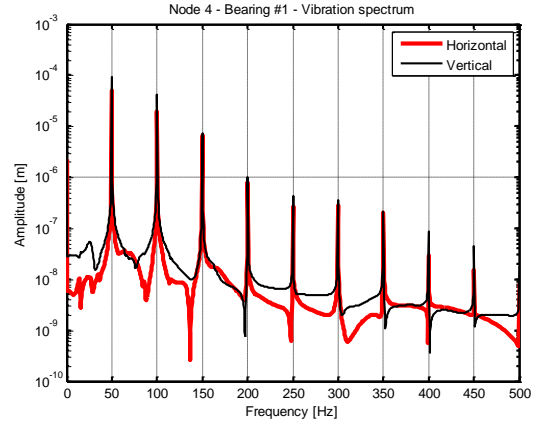


Fig. 8. Vibration spectrum, Brg. #1, 100 μm @ 90°, Ang. Mis. 15 mrad @ 0°.

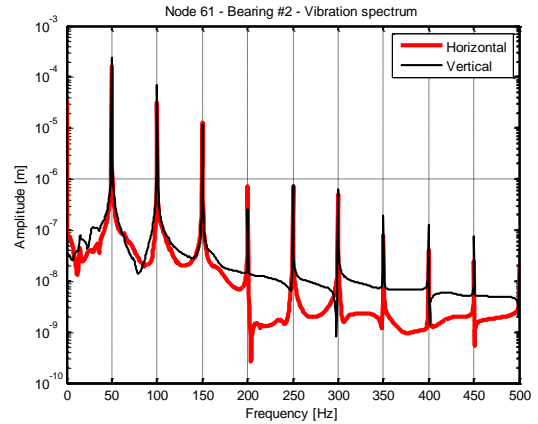


Fig. 9. Vibration spectrum, Brg. #2, 100 μm @ 90°, Ang. Mis. 15 mrad @ 0°.

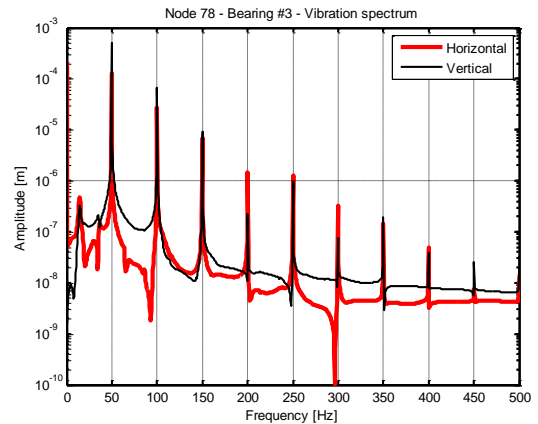


Fig. 10. Vibration spectrum, Brg. #3, 100 μm @ 90°, Ang. Mis. 15 mrad @ 0°.

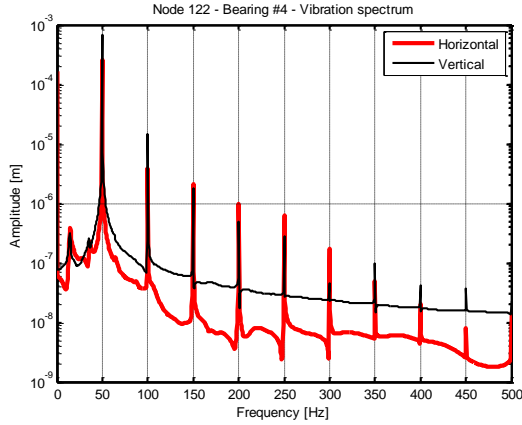


Fig. 11. Vibration spectrum, Brg. #4, 100 μm @ 90° , Ang. Mis. 15 mrad @ 0° .

Effect of radial misalignment

As it has been shown in the previous section, the model is able to consider simultaneously both radial and angular misalignment, with arbitrary combination of amplitudes and phases, and to explain the arising of nonlinear effects. Anyhow, because of the infinite possible combinations of radial and angular misalignment, a comprehensive analysis is rather awkward. Thus, the effects of radial and angular misalignment are analysed separately, starting from the former one.

In order to have the evaluation of the “degree” of nonlinearity, the ratios between the super-harmonic component amplitudes and the synchronous one are considered.

Figures 12-14 show respectively 2X/1X, 3X/1X and 4X/1X ratios for increasing magnitudes of radial misalignment from 50 to 210 μm with phase of 0° , i.e. in phase with the unbalance, for the vibration measuring planes close to bearings from #1 to #4.

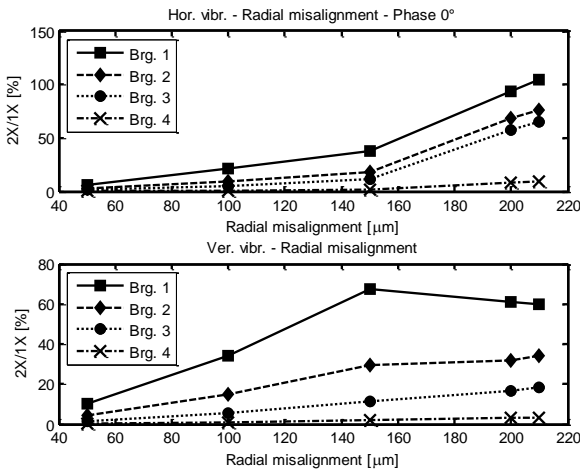


Fig. 12. Increasing magnitudes of radial misalignment @ 0° : 2X to 1X ratio.

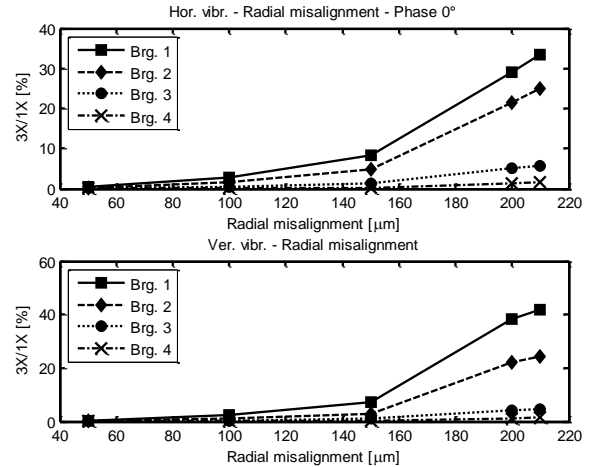


Fig. 13. Increasing magnitudes of radial misalignment @ 0° : 3X to 1X ratio.

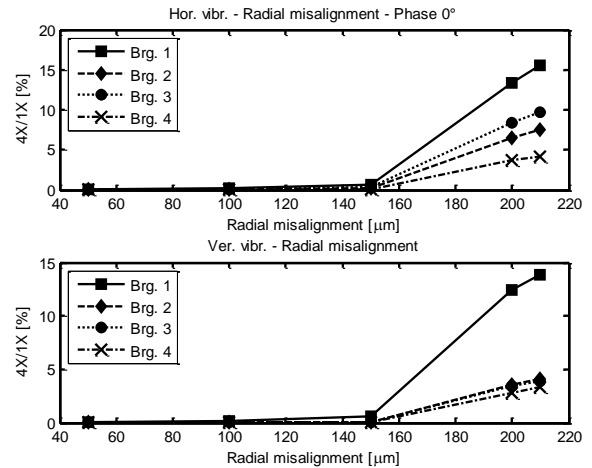


Fig. 14. Increasing magnitudes of radial misalignment @ 0° : 4X to 1X ratio.

With the exception of the 2X/1X ratio for vertical vibration in bearing #1, the ratios have more than linear increasing trends as a function of radial misalignment magnitude. The contributions of 4X components become significant only for high radial misalignment magnitude. 2X horizontal component becomes almost equal to 1X one when the misalignment is 210 μm .

For the considered machine model, if the radial misalignment is considered in quadrature to the unbalance, the increasing of the ratios becomes quicker than in the case of 0° phase, as shown in Fig. 15 for the 2X/1X ratio. In this case, 2X amplitude is about equal to 1X amplitude in horizontal and about one and half in vertical, when the misalignment is 100 μm . Similar results, in terms of quicker increasing when

the misalignment phase is 90° , are obtained for $3X/1X$ and $4X/1X$, but are not shown for the sake of brevity.

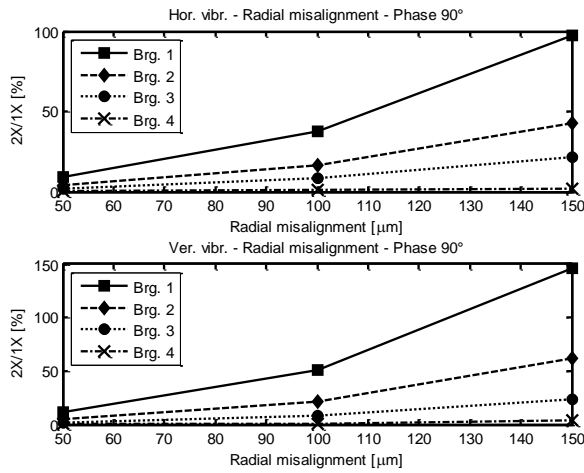


Fig. 15. Increasing magnitudes of radial misalignment @ 90° : 2X to 1X ratio.

Effect of angular misalignment

The effect of increasing magnitude of angular misalignment from 5 to 35 mrad with phase of 0° is shown in Figs. 16-18. Also in this case, nonlinear effects are evident. Even if the direct vibrations, corresponding to the maximum value of the angular misalignment considered, are comparable to those of the maximum values of radial misalignment, the ratio of the super-harmonics components to 1X component are much greater.

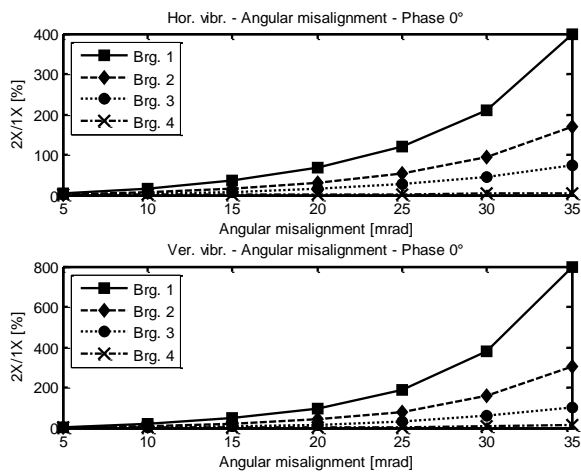


Fig. 16. Increasing magnitudes of angular misalignment @ 0° : 2X to 1X ratio.

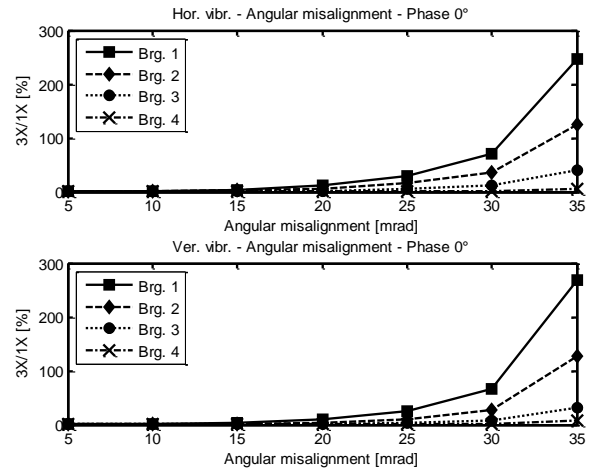


Fig. 17. Increasing magnitudes of angular misalignment @ 0° : 3X to 1X ratio.

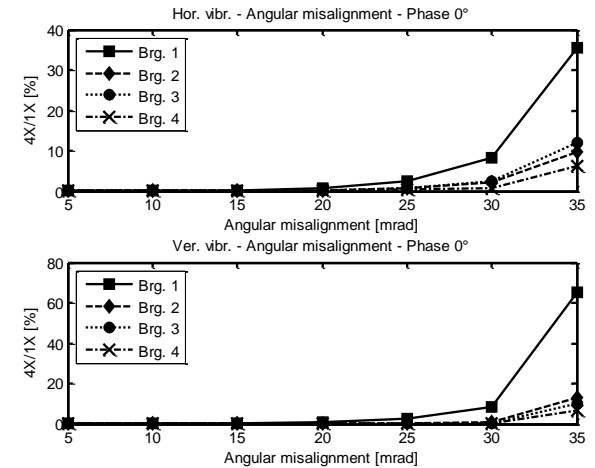


Fig. 18. Increasing magnitudes of angular misalignment @ 0° : 4X to 1X ratio.

CONCLUSIONS

Several studies in literature deal with rotor misalignment, but it looks like that this term is used to indicate different physical processes. In the paper, the authors have dealt with rigid coupling misalignment of a hyperstatic shaft-line equipped with journal bearings. A general model, which is able to consider every kind of rotating machines, has been presented in detail and used to perform some simulations. It has resulted that rigid coupling misalignments, in both radial and angular, and these combined, have generated nonlinear effects and the lateral vibration have resulted affected by super-harmonic components.

REFERENCES

[1] Muszyńska A., 2005, *Rotordynamics*, Taylor & Francis Group - CRC Press book, New York, USA.

- [2] Bou-Säïd B., Nicolas D., 1992, "Effect of misalignment on static and dynamic characteristics of hybrid bearing", *Tribology Transactions*, **35**(2), pp. 325-311.
- [3] Bently D.E., 2002, *Fundamentals of Rotating Machinery Diagnostics*, Bently Pressurized Bearings Press, Minden, NV, USA.
- [4] Xu M., Marangoni R.D., 1994, "Vibration analysis of a motor-flexible coupling-rotor system subject to misalignment and unbalance, Part I: Theoretical model and analysis", *Journal of Sound and Vibration*, **176**(5), pp. 663-679.
- [5] Xu M., Marangoni R.D., 1994, "Vibration analysis of a motor-flexible coupling-rotor system subject to misalignment and unbalance, Part II: Experimental validation", *Journal of Sound and Vibration*, **176**(5), pp. 681-691.
- [6] Sekhar A.S., Prabhu B.S., 1995, "Effects of coupling misalignment on vibrations of rotating machinery", *Journal of Sound and Vibration*, **185**(4), pp. 655-671.
- [7] Gibbons C.B., 1979, "Coupling Misalignment Forces", *Proc. of 5th Turbomachinery Symposium*, Texas A&M University, College Station, USA, pp. 111-116.
- [8] Lee Y.-S., Lee C.-W., 1999, "Modelling and vibration analysis of misaligned rotor-ball bearing systems", *Journal of Sound and Vibration*, **224**(1), pp. 17-32.
- [9] Hu W., Miah H., Feng N.S., Hahn E.J., 2000, "A Rig for Testing Lateral Misalignment Effects in a Flexible Rotor Supported on Three or More Hydrodynamic Journal Bearings", *Tribology International*, **33** (3-4), pp. 197-204.
- [10] Al-Hussain K.M., Redmond I., 2002, "Dynamic response of two rotors connected by rigid mechanical coupling with parallel misalignment", *Journal of Sound and Vibration*, **249**(3), pp. 483-498.
- [11] Al-Hussain K.M., 2003, "Dynamic stability of two rigid rotors connected by a flexible coupling with angular misalignment", *Journal of Sound and Vibration*, **266**(2), pp. 483-498.
- [12] Lees A.W., 2007, "Misalignment in rigidly coupled rotors", *Journal of Sound and Vibration*, **305**(1-2), pp. 261-271.
- [13] Tsai C.-Y., Huang S.-C., 2009, "Transfer matrix for rotor coupler with parallel misalignment", *Journal of Mechanical Science and Technology*, **23**(5), pp. 1383-1395.
- [14] Bahaloo H., Ebrahimi A., Samadi M., 2009, "Misalignment Modeling in Rotating Systems", *Proceedings of ASME Turbo Expo 2009: Power for Land, Sea and Air*, GT2009, June 8-12, 2009, Orlando, Florida, USA, paper GT2009-60121, pp. 1-7.
- [15] Lalanne M., Ferraris G., 1998, *Rotordynamics Predictions in Engineering*, John Wiley & Sons Inc., Chichester, England.
- [16] Childs D.W., 1993, *Turbomachinery Rotordynamics*, John Wiley & Sons Inc, Chichester, England.
- [17] Wowk V., 2000, *Machine Vibration: Alignment*, Mc Graw-Hill, New York.
- [18] Bachschmid N., Pennacchi P., Vania A., 2002, "Identification of Multiple Faults in Rotor Systems", *Journal of Sound and Vibration*, **254**(2), pp. 327-366.
- [19] Someya T., 1989, *Journal-Bearing Databook*, Springer-Verlag, Berlin, Germany.
- [20] Stachowiak G.W., Batchelor A.W., 2005, *Engineering Tribology*, Butterworth Heinemann, Burington, USA.
- [21] Pennacchi P., Bachschmid N., Vania A., Zanetta G.A., L. Gregori, 2006, "Use of Modal Representation for the Supporting Structure in Model Based Fault Identification of Large Rotating Machinery: Part 1 – Theoretical Remarks", *Mechanical Systems and Signal Processing*, **20**(3), pp. 662-681.